Recombination-pumped triatomic hydrogen infrared lasers

R. J. Saykally,[1] E. A. Michael,[1,a)] J. Wang,[2] and Chris H. Greene[2]
[1]*Department of Chemistry, University of California, Berkeley, California 94720-1460, USA*
[2]*Department of Physics and JILA, University of Colorado, Boulder, Colorado 80309-0440, USA*

(Received 6 May 2010; accepted 28 October 2010; published online XX XX XXXX)

Mid-infrared laser lines observed in hydrogen/rare gas discharges are assigned to three-body recombination processes involving an electron, a rare gas (He or Ne) atom, and the triatomic hydrogen ion (H_3^+). Calculations of radiative transitions between neutral H_3 Rydberg states support this interpretation, and link it to recent results for hydrogenic/rare gas afterglow plasmas. A mechanism for the population inversion is proposed, and the potential generality and astrophysical implications of such molecular recombination laser systems are briefly discussed. © *2010 American Institute of Physics*. [doi:10.1063/1.3518366]

I. INTRODUCTION

In 2001, Michael *et al.* reported the laboratory observation of extensive mid-IR laser action in water molecules excited in a dilute supersonically expanding He/H_2O plasma (Fig. 1), discovered accidentally while attempting to perform IR cavity ringdown absorption spectroscopy measurements[1,2] on supersonically cooled ions. From analysis of those data, and from similar observations of stimulated emission in the terahertz region,[3] we suggested that dissociative electron-ion recombination processes involving protonated water ions $[H_3O^+(H_2O)_n]$ were responsible for generating the requisite population inversions.[4] Interestingly, strong water IR emission from several massive star forming regions is observed[5–7] in this same region of the spectrum, currently modeled in terms of high temperature shock excitation, albeit with considerable uncertainty.

Subsequently,[8] we observed similar laser action at wavelengths near 7 microns in laboratory hydrogen/rare gas supersonic plasmas. These experiments and detailed theoretical calculations from Wang and Greene[9] suggest assignment to the metastable H_3 Rydberg molecule, generated "from the top down" by recombination of the ubiquitous H_3^+ molecular ion with low-energy electrons. Studies of flowing afterglow plasmas by Glosik *et al.*[10] suggest a three-body "collision assisted recombination" mechanism, rather than a simple two-body process because of the high ($>10^{14}$ cm^{-3}) gas density obtaining in the supersonic discharge source.

The neutral triatomic hydrogen Rydberg molecule (H_3) has been studied extensively by both experiment and theory since Herzberg first discovered its emission spectra in the 80s, and assigned the observed lines to transitions between the $n = 2$ and $n = 3$ Rydberg states.[11–14] The ground electronic state of this molecule is unbound, but singly excited (Rydberg) states are metastable, ultimately decaying either radiatively (with lifetime proportional to n^3) or by predissociation. These states could also autoionize, as an alternative decay mechanism, but this is comparatively unlikely for polyatomic species and will be neglected in the present exploratory analysis. Higher Rydberg states and ionization potentials of H_3 were later investigated and characterized.[15,16]

A crucial property of H_3 that has received extensive attention is its role as an intermediate in the dissociative recombination (DR) process, $H_3^+ + e^- \rightarrow H_2 + H$ or $H + H + H$. The large discrepancy between DR rates determined by experiment and theory has been resolved only recently through a combination of improved experimental techniques and theoretical advances incorporating the nonadiabatic Jahn–Teller effect (JTE) into the description.[16–19] The JTE, which also plays an important role in the photofragmentation process,[19,20] is a non-Born–Oppenheimer effect that engenders strong coupling between the electronic, vibrational, and rotational degrees of freedom. Hence, H_3 is also an important prototype for testing modern theoretical methods describing the complex dynamics of polyatomic Rydberg systems, as it is the simplest such molecule. The studies described here provide a novel way to probe H_3 and other such Rydberg molecules and their associated dynamics, and may thus comprise a useful advance in molecular physics.

In this paper, we describe our exploratory studies of these radiative processes involving metastable H_3 molecules generated via recombination of H_3^+ with electrons in a supersonically expanding plasma.[4,10] While atomic masers, particularly H-atom masers, generated by electron-ion recombination, are well known and comprise important probes of stellar and interstellar environments,[21] molecular analogues of these IR recombination-pumped lasers have apparently not been reported before our work.[4]

II. EXPERIMENT

The Berkeley spectrometer used to produce and measure IR laser transitions generated in supersonic plasmas is sketched in Fig. 2. Laser emission lines were produced from an ultrahigh finesse optical supercavity containing a supersonically expanding plasma in the spectral range of 930–4370 cm^{-1}, with the majority occurring near 7 μm (1430 cm^{-1}). The supersonic slit expansion generates a weakly ionized

[a)]Present address: Department of Electrical Engineering, Universidad de Chile, Santiago 6513027, Chile.

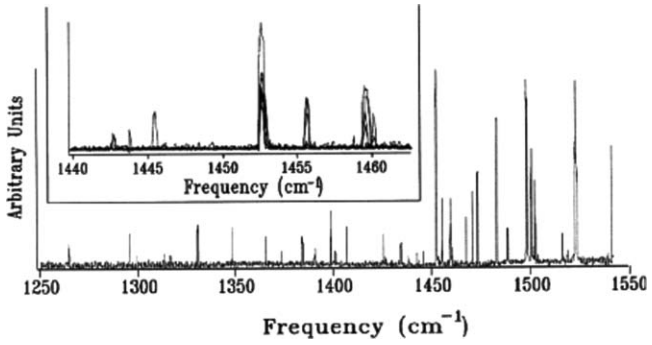

FIG. 1. Stick spectrum of the 38 lasing transitions measured in a dilute H_2O/He supersonically expanding plasma between 1200 and 1550 cm^{-1}. The strongest lines exhibit a signal to noise ratio > 2000. The inset shows actual measured spectra between 1440 to 1460 cm^{-1}, made at 10 different settings of the supercavity length. From Ref. 4.

plasma with neutral gas density expanding as the reciprocal of distance from the slit nozzle, such that the pressure in the region of observation is in the range of 0.1 to 10 Torr (densities of 10^{15}–10^{17} cm^{-3}). Fifty-seven laser transitions were observed in both H_2–He and H_2–Ne gas mixtures. Twenty-nine laser transitions in H_2–He were also observed in H_2O–He or H_2O–Ne discharges, which is not surprising, as these plasmas are known to produce significant amounts of hydrogen.[22]

Our studies[4,5,8] of similar supersonic plasmas and associated optical processes involving dilute H_2O/rare gas mixtures, wherein a set of laser transitions (given in Table I) were found to be produced only in such mixtures (i.e., disappeared when H_2 or O_2 was added), indicated a molecular ion rotational temperature near 100 K and a vibrational temperature near 2000 K at the pressures (100 Torr) prevailing in the active region of the discharge. It was found that laser intensity was highly dependent on partial pressure of H_2 in the expanding gas mixture, maximizing when the mixing ratio was <1%. No lasing was observed when pure H_2 gas was used for the expansion. This most probably reflects the conversion of the dominant H_3^+ ion to the H_5^+ complex at higher hydrogen concentrations, as characterized by Glosik *et al.*[23]

To test whether contaminants such as O_2 or H_2O could be involved in the lasing observed in the H_2/He plasma, three experiments were performed. First, O_2 was carefully added to the gas line through a needle valve to determine how the presence of O_2 affected laser intensity, revealing that it decreased significantly when O_2 was added to the gas mixture. Second, no lasing was observed when the H_2 cylinder was closed, indicating that the lasing species was indeed generated from the cylinder gas. Third, in case the cylinder was itself contaminated with traces of condensibles, the gas was flowed through a long (~8 ft) liquid nitrogen trap. No difference was observed in the lasing intensity with or without the liquid N_2 trap, indicating that the lasing species originates from species produced from pure H_2 and He or Ne.

The IR monochromator was manually scanned and the grating position, as well as the intensity, was recorded manually for all emission lines. Once a laser line was found, the piezo voltage was adjusted to modulate the cavity length and the signal maximum across the entire piezo range was recorded. The maximum signal was observed multiple times across the piezo range, which indicated that the cavity length modulation exceeded the emission wavelength. Some laser lines were more sensitive to cavity length than others, and a difference in piezo voltage of ~10% of the maximum value was sufficient to totally extinguish the most sensitive laser lines. Many laser lines were therefore missed on each scan of the monochromator, so many scans were done at many different piezo voltages to ensure that most laser transitions were detected. Cavity drift over the time required to scan the monochromator hindered reproducible observation of laser transitions. As a result, the list of laser lines measured in these preliminary experiments is certainly incomplete. In addition, the intensity of the laser lines varied between measurements and was extremely dependent on the piezo voltage, discharge voltage, cavity mirror alignment, and gas composition. Therefore, the relative intensities of the lines should not be considered quantitative.

A stick spectrum of the measured lines is given in Fig. 3. An expanded view of the 7 μm region illustrates the

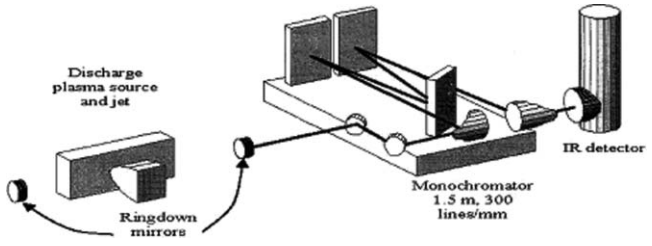

FIG. 2. Experiment for measuring the supersonic discharge laser emission. Laser emission was coupled out of the supercavity formed by a pair of supermirrors with > 0.9999 reflectivity at 8.0 μm, contained in a vacuum chamber (not shown) employing the mirrors as windows and evacuated by a high throughput roots pump system which maintains a chamber pressure near 20 mTorr. A pulsed supersonic discharge was produced by applying a 400–1200 V potential across the supersonic expansion just downstream of the 10 cm pulsed slit source operating with ca. 1 μs pulses at 40 Hz, as described in Ref. 4. The supermirror opposite the monochromator (JY TH 1500 with a 300 line/mm grating; spectral resolution of 0.05–0.09 cm^{-1}) was mounted on a piezoelectric translator, which could be adjusted to modulate the laser cavity length. The system was calibrated by observing known laser lines of CO and CO_2. Estimated error for all laser frequencies is ± 0.25 cm^{-1}.

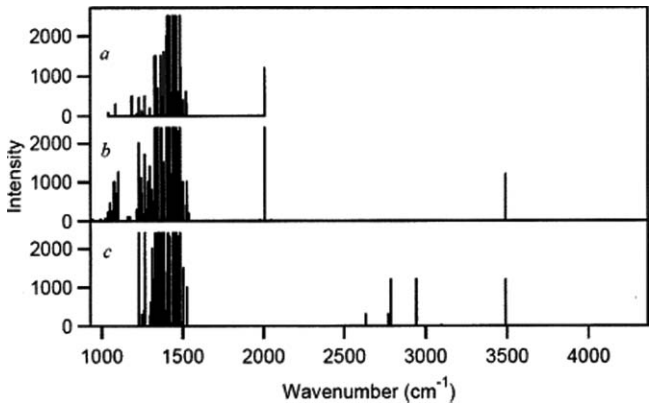

FIG. 3. Laser emission lines observed for plasmas generated in dilute hydrogen-containing gas mixtures: (a) H_2O seeded into Ne carrier gas, (b) H_2O seeded into He carrier gas, and (c) H_2 seeded into He carrier gas.

TABLE I. Mid-IR laser lines (cm^{-1}) observed in this work and their relative intensities (arbitrary units). The uncertainty of the measured lines is less than 0.05 cm^{-1}.

H_2–RG		H_2O–He		H_2O–Ne		Previously observed H_2O laser lines[a]
Laser line	Intensity	Laser line	Intensity	Laser line	Intensity	
						836.1
						845.3
		929.283	10			
		943.597	50			
		985.166	10			
		994.295	40			
		1022.02	60			
		1029.37	25			
		1032.31	80			
		1040.07	230			
				1044.22	80	
						1045.22
		1050.57	130			
		1052.14	450			
		1054.63	130			
						1055.44
		1063.75	250			
						1064.53
		1078.22	1000			
		1082	100			
				1086.04	300	
		1091.24	700			
		1103.27	1250			
		1163.07	100			
		1175.8	100			
				1186.71	500	
				1216.88	50	
		1218.47	300			
		1230.08	400			
		1230.63	400			
		1231.59	2000			
				1231.61	450	
1231.69	2400					
		1241.51	350			
		1241.99	600			
		1244.9	1100			
		1249.37	700			
				1249.4	120	
1249.5	300					
		1254.13	110			
				1258.98	50	
1262	400					
		1264.08	200			
1266.36	2400					
				1266.4	500	
		1266.44	1700			
		1272.69	300			
		1275.84	60			
		1285.93	1000			
		1287.88	250			
		1289.43	250			
						1292
1296.95	250					
						1297.19
		1297.83	1400	1297.83	200	
		1301.31	650			

TABLE I. Continued

H_2–RG		H_2O–He		H_2O–Ne		Previously observed H_2O laser lines[a]
Laser line	Intensity	Laser line	Intensity	Laser line	Intensity	
1301.34	600					
		1312.26	800			
1312.29	2000					
						1316.38
						1317
1317.38	1200					
		1317.49	500			
						1326
		1332.05	2400			
1332.17	2400			1332.17	1500	
1332.4	1500					
		1336.66	1000			
1337.94	400					
1340.17	150					
						1340.7
						1342
						1347
		1348.07	2400			
				1348.09	600	
1348.1	2400					
		1349.14	500			
				1349.66	200	
1349.71	1100					
				1349.84	700	
		1349.85	1500			
						1353
1356.63	2400					
				1355.95	20	
		1360.04	25			
				1367.17	1500	
		1367.29	2300			
1367.32	2400					
1367.53	1600					
				1368.46	500	
		1368.51	2400			
1368.63	2400					
						1371
		1371.18	10			
						1373
				1375.23	100	
1375.29	800					
		1375.35	300			
1375.91	60					
		1385.87	1500			
1385.9	2400					
				1385.96	1600	
1386.25	350					
						1388
1389.72	80					
		1392.6	40			
1396.61	150					
1398.69	400					
		1400.55	80			
		1401.13	2400			
				1401.15	2000	
1401.29	1400					
1401.77	50					
				1402.6	1200	

TABLE I. Continued

H_2–RG		H_2O–He		H_2O–Ne		Previously observed H_2O laser lines[a]
Laser line	Intensity	Laser line	Intensity	Laser line	Intensity	
				1403.27	500	
		1403.42	60			
1404	60					
		1407.2	10			
				1409.72	2500	
		1409.74	2400			
1409.93	2400					
						1410
		1410.97	1800			
		1418.84	2300			
				1418.92	2500	
1419.14	2300					
				1420.93	2100	
		1421.09	2400			
		1427.7	1200			
		1429.78	500			
				1436.47	600	
1437.05	80					
				1440.4	2500	
		1440.54	2400			
1440.61	2400					
1441.32	200					
		1444.22	500			
				1444.93	20	
				1447.71	2100	
		1447.85	2400			
1453.37	2400					
				1455.05	2500	
1455.24	2400					
		1455.45	2400			
1455.97	250					
				1458.15	20	
1458.3	80					
1459	8					
				1462.06	2500	
		1462.08	2400			
1462.32	2400					
				1469.98	40	
		1472.73	125			
				1473.21	600	
		1473.27	2300			
1473.55	2300					
1474.19	100					
1478.77	20					
				1485.47	2500	
		1485.57	2400			
1485.75	2400					
1486.55	350					
				1486.66	700	
		1487.09	1000			
		1490.76	200			
				1491.02	1200	
1492.3	100					
				1500.77	400	
1500.81	175					
		1500.81	1000			
1501.37	600					

TABLE I. Continued

H_2–RG		H_2O–He		H_2O–Ne		Previously observed H_2O laser lines[a]
Laser line	Intensity	Laser line	Intensity	Laser line	Intensity	
1501.92	20					
				1503.43	400	
		1503.81	300			
1503.85	1500					
				1521.31	600	
		1521.86	400			
				1525.88	300	
1526.32	1000					
		1526.39	1000			
		1537.44	200			
		1979.63	20			
		1983.19	20			
		2007.56	2400			
				2007.66	1200	
		2045.48	20			
						2096
2629.71	300					
2771.29	300					
2786.33	1200					
		2910.04	4			
2945.29	1200					
3100.05	30					
3491.73	1200					
		3491.73	1200			
4367.04	4					
		4367.04	4			
						4387.6

[a]From Ref. 26.

high density of laser lines observed in that region (Fig. 4). Outside of the indicated region, only two transitions (3491.7 and 4367.0 cm^{-1}) matched between the H_2O–He and H_2–He spectra. Table I lists the wavenumbers of all observed laser lines.

Wang and Greene[9] applied a long-range multipole potential model to the *d*-wave Rydberg states of H_3, used previously to characterize the Rydberg states of H_2 having high orbital angular momentum.[20,24] This formalism includes the perturbation between levels of different *n* (principal quantum number) and *l* (angular momentum quantum number) and $\{N^+, K^+\}$ (different ionic rotational levels) in a systematic fashion through the formalism of multichannel quantum-defect theory (MQDT). While the *d*-wave Rydberg states of H_3 were computed with this long-range model, the *p*-wave Rydberg states are computed separately, since they are mainly dominated by the short-range interaction between the outer electron and the ion core.[19,20] These *p*-wave Rydberg states either autoionize or predissociate much more rapidly than do the *d*-wave Rydberg states because of their stronger Jahn–Teller couplings, or through ordinary *l*-uncoupling, which causes rotational autoionization and does not rely on the Jahn–Teller effect. The corresponding *d*-*p* H_3 dipole transitions thereby satisfy one of the "golden rules of astrophysical lasers," viz. "the lifetime of the lower level of a lasing transition should be much shorter than the lifetime of the upper level independent of the excitation mechanism;"[25] hence, a population inversion can be created by the recombination process, and mid-IR lasing can occur under proper conditions. Comparison of the measured lasing lines with the theoretical *nd to np* lines suggests that metastable H_3 created in the expanding plasma is indeed a likely candidate for the carrier of these lasing transitions. Note, however, that the candidate lasing lines calculated in this study are primarily of the type 4*d*-4*p*, whereas

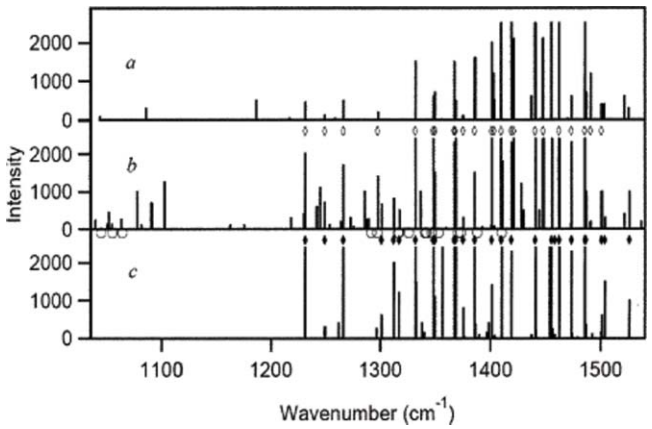

FIG. 4. Expanded view of the 7 μm region, indicating laser emission lines observed in both H_2O–He and H_2O–Ne discharges (open diamonds), as well as lines observed from the both H_2 and H_2O (He and Ne) mixtures (solid diamonds). Previously observed H_2O lasers from flow-cell discharge measurements are also indicated (open circles).

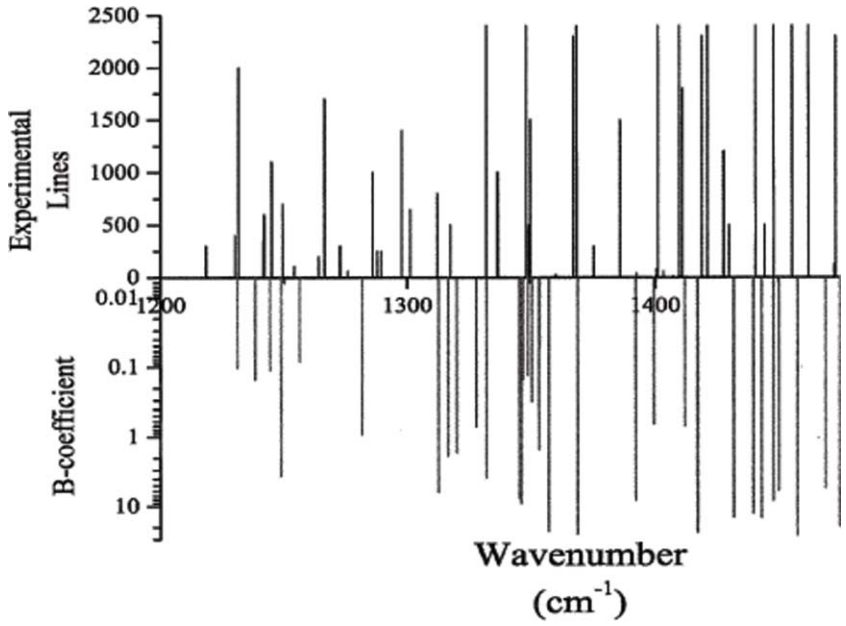

FIG. 5. Comparison of experimental results with calculated nd -> $n'p$ transitions of H_3. The experimental laser strength is in arbitrary units with linear scale, while the present theoretical B-coefficients are in the units of 10^{22} (m/Js^2) on a logarithmic scale. The calculated line positions have a precision of about 13 cm^{-1}.

the ternary recombination mechanism is believed to predominantly produce much higher Rydberg levels with principal quantum numbers in the range $n \approx 40$–60 or even higher. This view of the process therefore requires a cascade, i.e., a decay of these highly excited nf levels to the 4d states, which then have a population inversion and are able to lase while decaying to the 4p levels of H_3.

Because there are no laboratory measurements of the 4d-4p transitions that appear to be the most likely candidates for the lasing lines reported here, the theoretical model has been tested[9] against the experimental 3d to 3p transitions of H_3 that were measured by Herzberg, showing good agreement (the rms error for 14 tabulated transitions is below 13 cm^{-1}).[11] A comparison between the current experiment and our theoretical calculation is shown in Fig. 5. However, there are a few residual experimental lines having no corresponding theoretical transition. These may correspond to Rydberg levels of the ion core with other {N^+, K^+}, although we do not have specific candidates in mind at this point.

III. DISCUSSION

A. Mechanism of observed IR lasing

The conditions obtaining in the pulsed supersonic slit jet plasma (Fig. 2) used to generate the observed IR laser action described here are similar to those employed by Glosik *et al.* in their studies of H_3^+ recombination in flowing afterglow plasmas.[10,23] The total gas pressure drops from the 1–2 atmosphere nozzle backing pressure as the reciprocal of distance from the 300–400 μm wide exit slit, yielding neutral gas densities of 10^{14}–10^{17} cm^{-3} in the regions probed. Typical fractional ionizations in such plasmas are $\sim 10^{-5}$. Studies of the H_3O^+ ion in similar pulsed slit jet discharges yielded number densities near 10^{10} cm^{-3} and a rotational temperature near 110 K for this ion.[3,4,27] Glosik *et al.* measured the temperature-dependent recombination rate of H_3^+ with electrons in recombination-limited He/Ar/H_2 plasmas at He densities of 0.5–6 $\times$ 10^{17} cm^{-3} and temperatures of 77–300 K. They identified three different behaviors of the measured recombination coefficient with respect to hydrogen content. For [H_2] $< 10^{12}$ cm^{-3} (or $<10^{-5}$ of the total gas density), it increases with increasing H_2 density and the spin states of H_3^+ are not equilibrated. For $10^{12} <$ [H_2] $< 5 \times 10^{13}$ cm^{-3}, the rate is independent of H_2 density and the ion is in thermal equilibrium. For [H_2] $> 10^{13}$ cm^{-3}, it again increases with increasing hydrogen density due to the conversion of H_3^+ to the H_5^+ complex,[23] which recombines very rapidly, but which apparently does not produce observable laser action in our experiments. Analysis of these data indicated that three-body recombination processes dominated over two-body processes at pressures of a few Torr (10^{16}–10^{17} cm^{-3}) and temperatures near 300 K, and that this ternary rate maximizes at temperatures of 130–170 K. Hence, we can reasonably conclude that the three-body recombination processes also dominate the ion loss in our recombination-limited supersonic plasmas. Glosik *et al.*[10,23] show that such processes are ca. 100 times faster than that previously described by Bates and Khare,[28] and they present a theoretical model for them. In this model, the resonant $H_3^+ + e^-$ complex (i.e., the highly excited ($n \approx 40$–60) H_3 Rydberg molecule), which efficiently decays back into the ion and electron via rotational autoionization, collides with a He atom during its lifetime, changing the l-state of the complex to higher, longer-lived values. In particular, the $l = 1(p)$ electronic states are strongly coupled to the ion core and autoionize rapidly, whereas $l \geq 2(d)$ states are much more long-lived. These l-changing collisions of the H_3 molecule thus produce the population inversion required for the laser action observed in our experiments.

TABLE II. Possible assignment of laser lines observed in this work. We calculate theoretical laser lines by using models described in Ref. 9. The experiment lines are chosen from the H_2O–He laser lines which are also observed in H_2–RG or H_2O–Ne experiments. B is the Einstein stimulated emission coefficient.

Initial[a] N^+,K^+,N,nd	Final[b] $K^+,N,n'p_\lambda$	Theory lines (cm^{-1})	Expt. (cm^{-1})	Difference[c] (cm^{-1})	B/10^{21} (m/Js^2)	Expt. intensity
3,1,3,5d	1,2,5$p_{\pi-}$	1053.41	1054.63	1.22	2.26	130
3,1,1,5d	1,2,5$p_{\pi-}$	1084.27	1082	−2.27	4.24	100
			1218.47			300
1,1,1,4d	1,2,4$p_{\pi+}$	1231.06	1231.59	0.53	0.10	2000
1,1,3,4d	1,2,4$p_{\pi+}$	1248.76	1249.37	0.61	3.71	700
1,0,1,7d	0,1,6p_π	1256.36	1254.13	−2.23	0.08	110
			1266.44			1700
3,1,3,6d	1,3,5p_σ	1293.94	1297.83	3.89	961.95	1400
3,1,2,6d	1,3,5p_σ	1302.57	1301.31	−1.26	0.44	650
1,0,2,4d	0,2,4p_π	1312.78	1312.26	−0.52	6.28	800
2,1,3,6d	1,2,5p_σ	1316.66	1317.49	0.83	16.11	500
1,1,1,6d	1,1,5p_σ	1332.07	1332.05	−0.02	3.90	2400
2,2,3,6d	2,2,5p_σ	1337.16	1336.66	−0.50	8.22	1000
2,1,3,7d	1,2,6$p_{\pi-}$	1346.83	1348.07	1.24	20.04	2400
2,1,1,7d	1,1,6p_π	1350.49	1349.14	−1.35	2.92	500
2,2,2,4d	2,2,4p_π	1350.74	1349.85	−0.89	8.40	1500
1,0,3,4d	0,2,4p_π	1368.81	1367.29	−1.52	25.12	2300
3,1,4,7d	1,3,6$p_{\pi-}$	1370.69	1368.51	−2.18	2.34	2400
3,1,3,7d	1,3,6$p_{\pi-}$	1371.75	1371.18	−0.57	5.78	10
3,1,2,7d	1,3,6$p_{\pi-}$	1377.14	1375.35	−1.79	0.08	300
2,2,3,4d	2,2,4p_π	1387.33	1385.87	−1.46	9.59	1500
1,1,1,4d	1,1,4p_π	1392.30	1392.6	0.30	8.12	40
1,1,1,4d	1,2,4$p_{\pi-}$	1399.42	1400.55	1.13	0.66	80
1,1,1,4d	1,1,4p_π	1392.30	1401.13	8.83	8.12	2400
1,1,1,4d	1,2,4$p_{\pi-}$	1399.42	1403.42	4.00	0.66	60
1,0,1,4d	0,2,4p_π	1411.91	1407.2	−4.71	0.70	10
			1409.74			2400
1,1,3,4d	1,2,4p_π	1417.11	1418.84	1.73	23.93	2300
			1421.09			2400
2,1,2,4d	1,2,4$p_{\pi+}$	1439.63	1440.54	0.91	19.17	2400
1,1,2,4d	1,1,4p_π	1442.93	1444.22	1.29	14.62	500
2,2,0,4d	2,1,4p_π	1445.25	1447.85	2.60	35.43	2400
1,0,2,4d	0,1,4p_π	1457.61	1455.45	−2.16	26.57	2400
2,1,1,4d	1,2,4$p_{\pi+}$	1469.15	1462.08	−7.07	5.42	2400
2,2,1,4d	2,1,4p_π	1471.77	1472.73	0.96	26.57	125
1,1,1,4d	1,0,4p_π	1475.02	1473.27	−1.75	19.68	2300

[a]The initial states, labeled by the quantum number N^+,K^+,N,nd.
[b]The final states, labeled by the quantum number $K^+,N,n'p_\lambda$. An additional + or − denotes the possible Jahn–Teller splitting of two p_π states: + (−) denotes the higher (lower) energy level.
[c]The difference between the theory lines and H_2O–He laser lines.

Glosik *et al.* have shown that in the low $H_3^+ + e^-$ collision energy regime, rotational excitation of the vibrational ground state of the ion core with $\{N^+, K^+\} = \{1,1\}$ produces long-lived Rydberg states most efficiently. Hence, the most likely product immediately following collision would be a highly excited (n = 40–60) p-wave Rydberg electron attached to a $\{N^+, K^+\} = \{2,1\}$ ion core. A subsequent collision of the H_3 neutral molecule with a rare gas atom changes the Rydberg electron angular momentum to a longer-lived, higher value, and/or the collision of the He atom with the H_3^+ core might deexcite the ion core, which would close the rotational autoionization decay route. Radiative cascade can then populate the 4d levels that are the primary lasing candidates in transitions to the 4p states. Hence, in the theoretical calculation, we include the transitions from a 4d electron attached to {2,1}, {1,1}, and {1,0} cores to the $n'p$ energy levels of H_3. Other transitions of the type $nf \rightarrow n'd$ and $ng \rightarrow n'f$ of H_3 have also been checked, but they do not appear to be connected with the present experimental results.

B. Astrophysical implications

In principle, any radiative process involving hydrogen may well be relevant to astrophysics. In the present case, the ostensible requirement of gas densities above 10^{14} cm^{-3} may seem to preclude the relevance of the reported H_3 inversion mechanism to astrophysical environments, particularly to interstellar molecular clouds. However, it is possible that such stimulated emission could occur in warm regions of high density, e.g., star forming regions, or perhaps even in primordial

(Population III) stars and in the first galaxies, wherein the requisite radiative cooling of the accreting hydrogen/helium gas is thought to be extremely inefficient due to the absence of heavy elements (C,O) which are responsible for the rapid cooling obtaining in secondary star formation.[29] Intense Rydberg H_3 recombination lasing transitions such as those described herein, but found at large redshifts, of course, could then provide a means of detecting primordial stars and galaxies. Moreover, collisional excitation of both the H_3^+ ion core and the Rydberg *d*-states could comprise a previously unrecognized cooling mechanism. Further study is clearly needed to explore such questions.

Finally, we suggest that it would be of interest to search for similar recombination-pumped laser transitions in other likely astrophysical Rydberg molecules, like NH_4 and CH_5, formed by recombination of the corresponding chemically stable molecular ions, which are thought to be abundant in interstellar clouds). Strong electronic transitions have been predicted to occur for several of these Rydberg molecules in the visible-near IR regon.[31]

ACKNOWLEDGMENTS

The Berkeley experiments were supported by grants from the AFOSR (Grant No. F49620-02-1-0416) and the Experimental Physical Chemistry Program of the NSF (Grant No. CHE-0650950). The Colorado group has received support from the NSF under Grant Nos. PHY-0427460 and PHY-0427376, and from the DOE Office of Science. We also thank V. Kokoouline for helpful discussions and for access to unpublished data and programs.

[1] J. B. Paul, R. A. Provencal, C. Chapo, E. Michael, A. Pettersson, and R. J. Saykally, "Infrared Cavity Ringdown Laser Absorption Spectroscopy of Transient Species in Pulsed Supersonic Expansions," presented at the ACS Symposium Series 720 on *Cavity-ringdown spectroscopy: an ultratrace-absorption measurement technique*, 1997.
[2] R. Casaes, R. Provencal, J. Paul, and R. J. Saykally, J. Chem. Phys. **116**, 6640 (2002).
[3] E. A. Michael, C. J. Keoshian, S. K. Anderson, and R. J. Saykally, J. Mol. Spectrosc. **208**, 219 (2001).
[4] E. A. Michael, C. J. Keoshian, D. R. Wagner, S. K. Anderson, and R. J. Saykally, Chem. Phys. Lett. **338**, 277 (2001).
[5] E. F. van Dishoeck, Annu. Rev. Astron. Astrophys. **42**, 119 (2004).
[6] E. Gonzalez-Alfonso, J. Cernicharo, E. F. van Dishoeck, C. M. Wright, and A. Heras, Astrophys. J. **502**, L169 (1998).
[7] E. F. van Dishoeck, C. M. Wright, J. Cernicharo, E. Gonzalez-Alfonso, T. de Graauw, F. P. Helmich, and B. Vandenbussche, Astrophys. J. **502**, L173 (1998).
[8] A. J. Huneycutt, Ph.D. Thesis, "Studies of Atmospheric and Interstellar Molecules Using Cavity Ringdown Spectroscopy," University of California, Berkeley, 2003.
[9] J. Wang and C. H. Greene, Phys. Rev. A **82**, 022506 (2010).
[10] J. Glosik, I. Korolov, R. Plasil, O. Novotny, T. Kotrik, P. Hlavenka, J. Varju, I. A. Mikhailov, V. Kokoouline, and C. H. Greene, J. Phys. B-At. Mol. Opt. **41**, 191001 (2008).
[11] G. Herzberg, Annu. Rev. Phys. Chem. **38**, 27 (1987).
[12] I. Dabrowski and G. Herzberg, Can. J. Phys. **58**, 1238 (1980).
[13] G. Herzberg and J. K. G. Watson, Can. J. Phys. **58**, 1250 (1980).
[14] G. Herzberg, J. Chem. Phys. **70**, 4806 (1979).
[15] M. Vervloet and J. K. G. Watson, J. Mol. Spectrosc. **217**, 255 (2003).
[16] H. Helm, Phys. Rev. Lett. **56**, 42 (1986).
[17] B. J. Mccall, A. J. Huneycutt, R. J. Saykally, T. R. Geballe, N. Djuric, G. H. Dunn, J. Semaniak, O. Novotny, A. Al-Khalili, A. Ehlerding, F. Hellberg, S. Kalhori, A. Neau, R. Thomas, F. Osterdahl, and M. Larsson, Nature **422**, 500 (2003).
[18] B. J. Mccall, A. J. Huneycutt, R. J. Saykally, N. Djuric, G. H. Dunn, J. Semaniak, O. Novotny, A. Al-Khalili, A. Ehlerding, F. Hellberg, S. Kalhori, A. Neau, R. D. Thomas, A. Paal, F. Osterdahl, and M. Larsson, Phys. Rev. A **70**, 052716 (2004).
[19] V. Kokoouline and C. H. Greene, Phys. Rev. A **69**, 032711 (2004).
[20] J. A. Stephens and C. H. Greene, J. Chem. Phys. **102**, 1579 (1995).
[21] Jonathan Weintroub, James M. Moran, David J. Wilner, Ken Young, Ramprasad Rao, and Hiroko Shinnaga, Astrophys J. **677**,1140 (2008).
[22] A. Fridman, *Plasma Chemistry* (Cambridge University Press, Cambridge, 2008).
[23] J. Glosík, O. Novotný, A. Pysanenko, P. Zakouril, R. Plašil, P. Kudrna and V. Poterya, Plasma Sources Sci. Technol. **12**, S117 (2003).
[24] G. Herzberg and C. Jungen, J. Chem. Phys. **77**, 5876 (1982).
[25] S. Johansson and V. S. Letokhov, New Astron. Rev. **51**, 443 (2007).
[26] B. Hartmann, B. Kleman, and G. Spangstedt, IEEE J. Quantum Electron., **QE-4**, 296 (1968), cited in M. J. Weber, *Handbook of Lasers* (CRC Press, Boca Raton, FL, 2001).
[27] R. A. Provencal, J. B. Paul, E. Michael, and R. J. Saykally, *Photonics Spectra* **32**, 159 (1998).
[28] D. R. Bates and S. P. Khare, Proc. Phys. Soc., 231 (1965).
[29] V. Bromm and R. B. Larson, Annu. Rev. Astron. Astrophys. **42**, 79 (2004).
[30] N. Yoshida, K. Omukai, and L. Hernquist, Science **321**, 669 (2008).
[31] S. Raynor and D. R. Herschbach, J. Phys. Chem. **86**, 3592 (1982).